

## Assessment of Severe Shot Peening on Surface Characteristics of Al Alloys

M. Guagliano<sup>1,2</sup>, S. Bagherifard<sup>2</sup>, I. Fernandez Parienete<sup>3</sup> and R. Ghelichi<sup>2</sup>

**Abstract:** Surface grain refinement is a relatively new process aimed to enhance mechanical material properties. In this study Al7075-T6 bars have been shot peened with parameters (shot speed and treatment duration) much stronger from those of conventional shot peening (SP). Residual stress state and microstructure gradient have been observed by means of transmission electron microscopy (TEM), X-ray diffraction (XRD) and nano indentation tester. Formation of a fine grained layer of material on top surface of the specimens was confirmed by TEM and also XRD measurements. XRD results show significant depth affected both in terms of residual stress and full width half maximum (FWHM). Measurements also indicate of notable improvements in cases of hardness and elastic modulus in comparison with untreated material.

The results obtained from different peening conditions are then critically discussed and compared. Findings imply that using optimized shot peening parameters, it would be possible to create a fine grained layer on surface of components and consequently increase fatigue life and any other properties affected by grain size.

**Keywords:** Surface nanocrystallization- Severe shot peening- Residual stresses- XRD measurements.

### 1 Introduction

In most cases material failures such as fatigue fracture, fretting fatigue, wear and corrosion originate from the exterior layers of the work piece. These phenomena are all extremely sensitive to the structure and properties of the material surface. Thus it seems of great industrial application to apply an approach to optimize the material properties on the surface of the part in order to enhance global behavior and service lifetime.

---

<sup>1</sup> Corresponding author: E-mail: mario.guagliano@polimi.it; Tel.: 02-2399-8206; Fax.: 02-2399-8202

<sup>2</sup> Department of Mechanical Eng., Politecnico di Milano, Via La Masa 34, 20156 Milan, Italy.

<sup>3</sup> Department of Material Science and Metallurgical Eng., University of Oviedo, Gijón, Spain.

On the other hand, fine grained materials are experiencing a rapid development in recent years due to their existing and potential applications in a wide variety of technological areas. These materials, structurally characterized by very fine grain size and large amounts of grain boundary volume, have proved to possess superior mechanical properties fundamentally different from their conventional coarse-grained polycrystalline counterparts [Cahn (1990); Morris (1998); Nagahora, Kita and Ohtera (1999); Kulik (2001)].

Thus it is naturally expected that the global performance can be enhanced when forming such a fine grained layer with superior properties on material surface without changing the chemical composition. Great efforts have been recently devoted to produce materials with nanostructured surface and coarse grained underlying layers owing to their highly improved mechanical properties. These processes actually combine superior properties of nanomaterials and conventional engineering materials in order to enhance the performance and service lifetime of the work piece.

SP is a considerably useful method to improve fatigue properties, avoid fretting, wear and stress corrosion cracking. The aim of SP process is the creation of compressive residual stresses close to the surface and the work hardening of the near surface layer of material. These effects are very useful in order to totally prevent or delay the failure of the part [Marsh (1993); Almen and Black (1963); Wagner (1999); Blarasin, Guagliano and Vergani (1997)]. There are lots of papers about the ability of SP to improve mechanical behavior of materials [Guagliano (2001); Guagliano, Riva and Giudetti (2002); Schulze (2006)]. Most of them affirm that the effect of shot peening is mainly related to the induced residual stresses, while the contribution of surface work hardening can be functional. Recent results show that in some cases surface hardening can be considered the main cause of the modified behavior of shot peened materials [Dai and Shaw (2007); Fernandez Pariente and Guagliano (2008)].

Till now different methods of shot peening have been aimed at achieving fine grained layers on the surface of treated parts. It has been reported that some of these methods which use shots with very high kinetic energy are capable of synthesis of ultrafine grained materials even in the nanometer scale on the surface layer of the specimens [Liu, Lu and Lu (2000); Liu, Fecht and Umemoto (2004); Todaka, Umemoto and Tsuchiya (2004)]. These diverse methods which are referred to as surface mechanical attrition treatment [Lu and Lu (2004); Ren, Shan, Zhang, Song, Liu (2006)], ultrasonic shot peening [Lu and Lu (1999); Kulik (2001)], high energy shot peening [Liu, Wang, Lou, Lu and Lu (2001)] and surface nanocrystallization and hardening (SNH) [Villegas, Dai and Shaw (2003) and (2005); Villegas, Dai, Shaw and Liaw (2005)], are somehow different from conventional method that is air blast shot peening (ABSP), in the needed technological facilities and also for

the mechanics of the treatment itself.

In a study performed on ultrasonic shot peening in which shot velocity has a wider distribution in comparison with ABSP and also has a random impact direction of shot to specimen while in ABSP impact direction is almost perpendicular, an average grain size of about 30 nm was obtained on Iron specimens when the treatment duration was between 50-450 s [Tao, Sui, Lu and Lu (1999)]. ultrasonic shot peening was applied in another research to 316L stainless steel specimens. The vibration frequency of the chamber driven by ultrasonic generator was set to 20 kHz and the shot diameter was 3 mm. After a processing duration of 30s, the average grain size in the surface layer was measured to be about 20 nm [Liu, Lu and Lu (2000)].

In another study pure iron plates were subjected to surface mechanical attrition treatment using steel balls (8 mm in diameter) vibrated by a generator repeatedly stroking sample surface. Repeated attrition induced severe plastic deformation of the surface and eventually nanocrystalline grains with an average size of about 200 nm developed therein [Tong, Liu, Wang, Tao, Wang, Zuo and He (2007)].

Low carbon steel specimens were treated by high energy shot peening which in principle is similar to ultrasonic shot peening but with a lower frequency and bigger shots. The entire surface of the specimens was peened by the high energy flying shots with a processing time of 1800s, nanograins with an average size of 33 nm were obtained on the surface layer [Liu, Wang, Lou, Lu and Lu (2001)].

Dai and Shaw [Dai and Shaw (2007)] applied SNH process to 5052 C-2000 alloy specimens using five tungsten carbide/cobalt (WC/Co) balls with a diameter of 7.94 mm which provided the desired impact on the surface of the specimen. The SNH treatment was conducted in argon atmosphere and lasted for 30 min. The velocity of the balls (5 m/s) in the SNH process was achieved by shaking the container three dimensionally. Surface characterization revealed that the nanograined surface layer was formed with an average grain size of 20 nm at the very impacted surface.

ABSP is a SP process through which the shots are projected by compressed air. The schematic of the equipment is illustrated in Figure 1. Typical characteristics of ABSP are: the shot velocity has a narrow distribution and the impact direction of shot to specimen is almost perpendicular. Air pressure, shot size and shot materials are the effectual factors to be investigated in ABSP. These are the process parameters that mainly affect the results of the treatment and the characteristic of the nanostructured surface. In ABSP, nanostructured surface layer is produced when higher shot speed and larger coverage than conventional operation are applied [Umemoto, Todaka, Watanabe, Li and Tsuchiya (2005)].

In this research, Aluminum specimens are treated by ABSP using the conventional SP device and applying an unconventional combination of peening parameters in

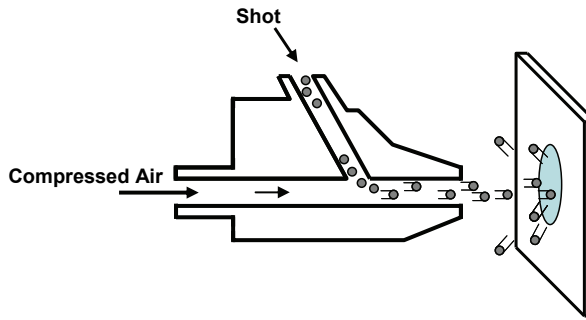


Figure 1: Schematic illustration showing the equipment of ABSP

order to multiply kinetic energy of the process. Results of this parameter modification which is aimed to generate nanograins in the surface layer of the specimen is then investigated in cases of residual stress state using XRD and also microstructure of treated parts using transmission electron microscopy (TEM).

## 2 Experimental procedure

Al7075-T6 bars (Al. alloy 7075) were subjected to two different approaches of air blast shot peening. Using cast steel shots, specimens were treated with particular combinations of SP parameters basically different from typical parameters used in industry for Al alloys. The alternative peening parameters are presented in Table 1 differentiated by specimen labels A and B.

Table 1: Aspects of the SP processes

Specimen label	A	B
Shot diameter [mm]	0.6	0.6
Air speed [m/s]	90	90
Almen Intensity [0.0001 inch]	7C	7C
Treatment time [s]	450	900

To study the state of residual stresses, XRD analysis of surface layer in the as-treated specimens was performed using an AST X-Stress 3000 X-ray diffractometer (Figure 2) (radiation Cr  $K\alpha$ , irradiated area  $1\text{mm}^2$ ,  $\sin^2\psi$  method, diffraction angles ( $2\theta$ ) scanned between  $-45$  and  $45$ ) with x-ray exposure time of 30 s. For obtaining the trend of residual stresses, measurements were carried out in depth step by step removing a very thin layer of material using an electro-polishing de-

vice. Grain size measurements were performed by another in situ high-energy synchrotron X-ray diffraction device to obtain grain size and microstrain.



Figure 2: AST X-Stress 3000 X-ray diffractometer used for residual stress measurements

Microstructure of the surface layer was observed by TEM using a Philips CM12 microscope operating at 120 kV. To perform TEM observations very thin pieces of specimens were first cut by electrical discharge machine (EDM) as shown in Figure 3, then were mechanically polished from the untreated side and finally the last step of thinning was performed by means of ion milling with proper incident angles.



Figure 3: View of the treated, untreated specimens and the slice cut by EDM

Hardness and elastic modulus were measured on treated surface using nano indentation tester (NHT).

### 3 Results and discussion

#### 3.1 XRD measurements

Distribution of macroscopic residual stresses on the plane parallel to the impacted surface determined by XRD is shown for the treated specimens in Figure 4. As shown in Figure 4, in both cases the maximum compressive residual stress is found to be under the surface, showing the common trend for shot peened specimens. The results also imply that a considerable depth of material is characterized with significant compressive residual stresses in both specimens.

It shall also be taken into consideration that due to very high kinetic energy of the peening process, the roughness over the surface of specimens is significant. The high points in the rough surface contribute more to the diffraction pattern and can consequently introduce some errors to the XRD measurements especially on the first layers [Cullity and Stock (2001)].

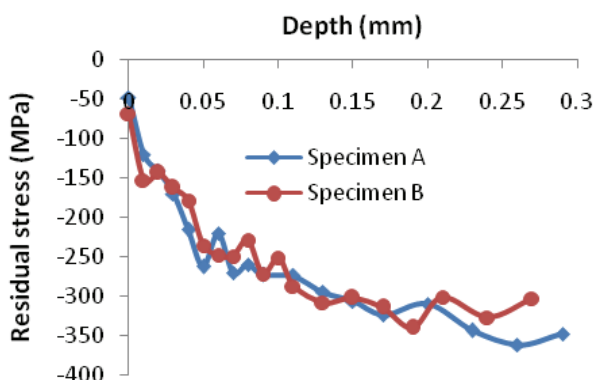


Figure 4: In plane residual stress profile as a function of position measured from impacted surface by XRD device.

Another parameter measured by X-ray diffraction, FWHM, that is the width of the diffraction peak at half the maximum intensity, is shown in Figure 5. It is measured as an index of hardening of material, and of the crystal size. As shown in Figure 5 maximum FWHM is observed on the surface of specimen, declining down to the depth. Increasing treatment time has produced very slight difference in the

results. It can be concluded that changing process time in this scale is not notably affecting state of residual stresses. In terms of FWHM in the surface region there is no considerable difference between the results for specimen A and B but getting farther from impacted surface FWHM values decrease more rapidly in specimen A. It seems that the thickness of the work hardened layer is more pronounced in specimen B and this can be attributed to increased process time.

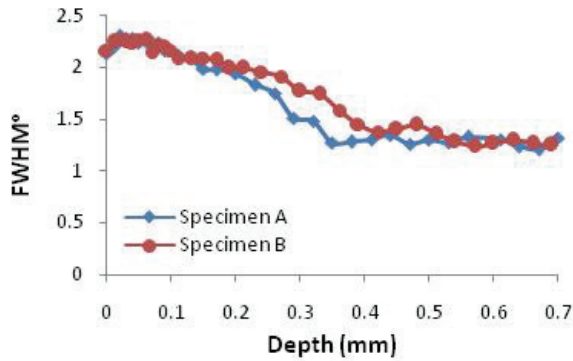


Figure 5: FWHM profile as a function of position measured from impacted surface by XRD device.

### 3.2 Nanohardness and elastic modulus measurement

Hardness and elastic modulus were measured on specimens surface using NHT device which is a machine especially suited to perform measurements on films with thickness in micrometer or lower scale. Various indentation matrixes have been performed on shot peened area of each specimen. The mean results of these measurements are listed in Table 2.

Table 2: Vickers hardness and elastic modulus measured for specimens A and B

	Vickers hardness [HV]	Elastic Modulus [GPa]
Specimen A	210	100
Specimen B	240	106
Typical values for Al7075	175	70

As shown in Tab.2 this unconventional SP process has lead to improvements up to 20% and 37% in hardness of specimens A and B respectively and also an enhancement of 30% in elastic modulus for both specimens. This happened because

the elastic limit or the yield strength is increased when the dislocation motion is retarded by grain boundaries [Wang and Li (2003)].

Comparing the results obtained for specimen A and B, it is approved that increasing SP time has lead to considerable increment of hardness but less change is observed in terms of elastic modulus.

### 3.3 Grain size measurements

XRD analyses were carried out for determining average grain size and microstrain in the surface layer.

Diffraction peaks of a Si internal standard sample were used as a reference, to represent the instrumental broadening. The experimental data were analyzed via MAUD program (Materials Analysis Using Diffraction) [Lutterotti, Matthies, Wenk, Schultz, and Richardson, (1997)], through Rietveld procedure using isotropic size-strain model [Rietveld (1969)]. The Rietveld method uses multiple reflections of experimental data and can determine structural and microstructural parameters (lattice parameters, atomic coordinates, thermal factors, crystallite size, microstrain and so on).

Figure 6 presents X-ray diffraction patterns of specimen B. For the top surface layer, evident broadening of Bragg diffraction peaks was seen owing to a grain refinement and increase in the atomic-level microstrain. The average grain size was found to be about 56 nm for specimen A and 53 for specimen B. Measured mean microstrain was 0.00208 (*r.m.s.*) and 0.00233 (*r.m.s.*) for specimen A and B respectively. Results indicate that grain size and internal strain introduced by this method of SP does not change remarkably with the processing time.

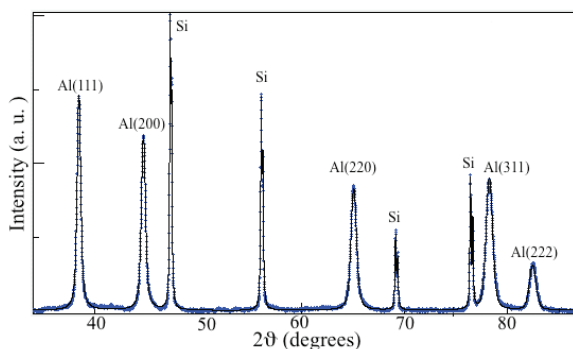


Figure 6: X-ray diffraction patterns of the specimen B



### 3.4 TEM observations

Figure 7 shows TEM bright-field image and the corresponding selected area diffraction pattern obtained at impacted surface of specimen A. The bright field image (Figure 7.a) represents irregularly shaped, anisotropic and elongated grains the average size of which is measured to be 50 nm. This mean size is close to the average grain size obtained from XRD measurement. It shall be underlined that even in the same depth it is not possible to obtain a sharp distribution of the grain size.

The selected area diffraction pattern (Figure 7.b) is composed of partially continuous diffraction rings, which confirm that the as-received large crystalline grains have been broken down to nanograins at this region. These diffraction patterns also clearly indicate that nanograins at impacted surface have completely random orientations with high-angle grain boundaries. Based on TEM observations, it can be observed that the nanostructured layer has a grain-size gradient as the locations moves from the impacted surface.

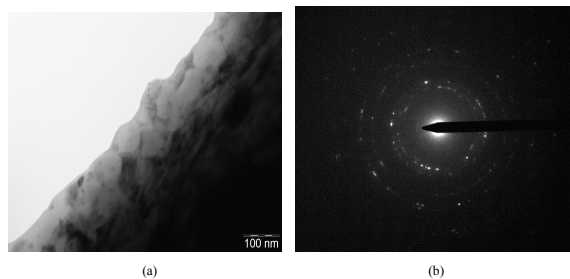


Figure 7: Plane-view TEM observations and grain size distributions of specimen A. a) bright-field image of the impacted surface showing the formation of nanograins; b) correspondent selected area diffraction pattern

## 4 Conclusions

Al7075 bars were treated by unconventional methods of air blast shot peening with very high kinetic energy aimed at generation of ultrafine grains on the surface layer of specimens. Experimental surface characterization of specimens has been performed by XRD measurements, TEM observations and nanohardness tests. In the light of the obtained results the following conclusions can be drawn:

- TEM and XRD observations confirm that a layer of material with elongated anisotropic nano grains has been created on surface of the specimens.

- According to measurements performed by nanohardness tester, the nanocrystallized layer shows increased hardness and modulus of elasticity.
- Trend of full width half maximum obtained from XRD measurements seems to follow the structure gradient from fine grained surface layer to coarse-grained bulk material.
- The unconventional shot peening process leads to a significant increase in the depth affected by residual stresses.
- Among the parameters selected to increase kinetic energy of the shots, treatment time at this scale seems to be not so effective in altering material properties in the top surface layer.

As a general point based on the experimental results it is concluded that the employed unconventional air blast shot peening process is a promising method to produce advanced materials for strength-intensive service applications showing potentially remarkable improvement in fatigue and fracture behavior which are greatly sensitive to grain size and the property of material on the surface of the part.

## References

- Almen, J. O.; Black, P.H.** (1963): *Residual stresses and fatigue in metals*, McGraw-Hill Publ. Company.
- Blarasin, A.; Guagliano, M.; Vergani, L.** (1997): Fatigue crack growth prediction in specimens similar to spur gear teeth, *Fatigue Fract. Engng. Mater. struct.*, vol. 20, pp. 1171-1182.
- Cahn, R.W.** (1990): Nanostructured materials, *Nature*, Vol. 348, pp.389-390.
- Cullity, B.D.; Stock, S.R.** (2001): *Elements of X-ray diffraction*, Prentice Hall Inc.
- Dai, K.; Shaw, L.** (2007): Comparison between shot peening and surface nanocrystallization and hardening processes, *Materials Science and Engineering A*, vol. 463, pp. 46–53.
- Dai, K.; Shaw, L.** (2008): Analysis of fatigue resistance improvements via surface severe plastic deformation, *International Journal of Fatigue*, vol. 30, pp. 1398-1408.
- Fernandez Pariente, I.; Guagliano, M.** (2008): About the role of residual stresses and surface work hardening on fatigue  $\Delta K_{th}$  of a nitrided and shot peened low-alloy steel, *Surface and Coating technology*, vol. 202, pp.3072-3080.
- Guagliano, M.** (2001): Relating Almen intensity to residual stresses induced by shot peening: a numerical approach, *Journal of Materials Processing Technology*,

vol. 110 pp. 277-286.

**Guagliano, M.; Riva, E.; Giudetti, M.** (2002): Contact fatigue failure analysis of shot-peened gears, *Engineering Failure Analysis*. Vol. 9, pp. 147-158.

**Kulik, T.** (2001): Nanocrystallization of metallic glasses, *J. Non-crystalline Solids*, vol. 287, pp. 145–161.

**Liu, G.; Lu, J.; Lu, K.** (2000): Surface nanocrystallization of 316 stainless steel induced by ultrasonic shot peening, *Materials Science and Engineering A*, vol. 286, pp. 91-95.

**Liu, G.; Wang, S.C.; Lou, X.F.; Lu J.; Lu, K.** (2001): Low carbon steel with nanostructured surface layer induced by high-energy shot peening, *Scripta Mater.* vol. 44 pp. 1791-1795.

**Liu, Z.G.; Fecht, H.J.; Umemoto, M.** (2004): Microstructural evolution and nanocrystal formation during deformation of Fe–C alloys, *Materials Science and Engineering A*, vol. 375–377, pp. 839-843.

**Lu, K.; Lu, J.** (1999): Surface nanocrystallization (SNC) of metallic materials—presentation of the concept behind a new approach, *J. Mater. Sci. Technol.* Vol. 15, pp. 193-197.

**Lu, K.; Lu, J.** (2004): Nanostructured surface layer on metallic materials induced by surface mechanical attrition treatment, *Materials Science and Engineering A*, vol. 375–377, pp. 38–45.

**Lutterotti, L.; Matthies, S.; Wenk, H.R.; Schultz, A.S.; Richardson, J.W.** (1997): Combined texture and structure analysis of deformed limestone from time-of-flight neutron diffraction spectra, *Journal of Applied Physics*, vol. 81, pp. 594.

**Morris, D.** (1998): *Mechanical behavior of nanostructured materials*, Clausthal, Germany: Trans. Tech. Publications Ltd.

**Marsh, K.J.** (1993): *Shot Peening: Techniques and Applications*, EMAS, London.

**Nagahora, J.; Kita, K.; Ohtera, K.** (1999): New type aluminum alloys with higher strength, *Mater. Sci. Forum*, vol. 304, pp. 825–829.

**Ren, J.; Shan, A.; Zhang, J.; Song, H.; Liu, J.** (2006): Surface nanocrystallization of Ni3Al by surface mechanical attrition treatment, *Materials Letters* vol. 60, pp. 2076–2079.

**Rietveld, H.M.** (1969): A profile refinement method for nuclear and magnetic structures, *Journal of Applied Crystallography*, vol. 2, pp. 65.

**Schulze, V.** (2006): *Modern Mechanical surface treatment*, Wiley-VCH.

**Tao, N.R.; Sui, M.L.; Lu, J.; Lu, K.** (1999): Surface nanocrystallization of Iron induced by ultrasonic shot peening, *NanoStructured materials*, vol.11-4, pp. 433-

440.

**Todaka, Y.; Umemoto, M.; Tsuchiya, K.** (2004): Comparison of Nanocrystalline surface layer in steels formed by Air Blast and Ultrasonic Shot peening, *Materials Transaction*, vol. 45, pp. 376-379.

**Tong, W.P.; Liu, C.Z.; Wang, W.; Tao, N.R.; Wang, Z.B.; Zuo, L.; He, J.C.** (2007): Gaseous nitriding of iron with nanostructured surface layer, *Scripta Materialia*, vol.57, pp. 533-536.

**Umemoto, M.; Todaka, Y.; Watanabe, Y.; Li, J.; Tsuchiya, K.** (2005): Comparison of nanocrystallization in steels by ball milling, shot peening and drilling, International Symposium on Metastable, Mechanically Alloyed and Nanocrystalline Materials, *Journal of Metastable and Nanocrystalline Materials*, vol. 24-25, pp. 571-576.

**Villegas, J.; Dai, K.; Shaw, L.** (2003): Surface roughness evolution in surface nanocrystallization and hardening (SNH) process. In: Srivatsan T, Varin R, editors. Processing and fabrication of advanced materials: XII. Materials Park, OH: ASM International, pp.358–372.

**Villegas, J.; Dai, K.; Shaw, L.** (2005): An analytical model of the surface roughness of an aluminum alloy treated with a surface nanocrystallization and hardening process, *Scripta Materialia*, vol. 52, pp. 259–263.

**Villegas, J.; Dai, K., Shaw, L.; Liaw, P.** (2005): Nanocrystallization of a nickel alloy subjected to surface severe plastic deformation, *Materials Science and Engineering A*, vol. 410–411, pp. 257–260.

**Wagner, L.** (1999): Mechanical surface treatments on titanium, aluminum and magnesium alloys, *Materials Science and Engineering A*, vol. 263, pp.210-216.

**Wang, L.; Li, D.Y.** (2003): Mechanical, electrochemical and tribological properties of nanocrystalline surface of brass produced by sandblasting and annealing, *Surface and Coating Technology*, vol.167, pp. 188-196.